Arylamine *N*-Acetyltransferase-1 Is Highly Expressed in Breast Cancers and Conveys Enhanced Growth and Resistance to Etoposide *in Vitro*

Paul J. Adam,[1] Joanne Berry,[1] Julie A. Loader,[1] Kerry L. Tyson,[1] Graham Craggs,[1] Paul Smith,[1] Jackie De Belin,[1] Graham Steers,[2] Francesco Pezzella,[2] Kris F. Sachsenmeir,[3] Alasdair C. Stamps,[1] Athula Herath,[1] Edith Sim,[5] Michael J. O'Hare,[4] Adrian L. Harris,[2] and Jonathan A. Terrett[1]

[1]Oxford Glycosciences, Abingdon, Oxon, United Kingdom; [2]Cancer Research UK Molecular Oncology Laboratories, Weatherall Institute of Molecular Medicine, John Radcliffe Hospital, Oxford, United Kingdom; [3]Automated Cell Inc., Pittsburgh, PA; [4]Department of Surgery, Ludwig Institute for Cancer Research/University College London Breast Cancer Laboratory, London, United Kingdom; and [5]Department of Pharmacology, University of Oxford, Oxford, United Kingdom

Abstract

Comparative two-dimensional proteome analysis was used to identify proteins differentially expressed in multiple clinical normal and breast cancer tissues. One protein, the expression of which was elevated in invasive ductal and lobular breast carcinomas when compared with normal breast tissue, was arylamine *N*-acetyltransferase-1 (NAT-1), a Phase II drug-metabolizing enzyme. NAT-1 overexpression in clinical breast cancers was confirmed at the mRNA level and immunohistochemical analysis of NAT-1 in 108 breast cancer donors demonstrated a strong association of NAT-1 staining with estrogen receptor-positive tumors. Analysis of the effect of active NAT-1 overexpression in a normal luminal epithelial-derived cell line demonstrated enhanced growth properties and etoposide resistance relative to control cells. Thus, NAT-1 may not only play a role in the development of cancers through enhanced mutagenesis but may also contribute to the resistance of some cancers to cytotoxic drugs.

Introduction

Breast cancer is the most frequently diagnosed cancer in women and accounts for 30% of all cancers diagnosed in the United States (1). Although the implementation of screening programs for the early detection of breast cancer and the development of chemotherapy, radiotherapy, and anti-estrogen therapies have improved the survival of breast cancer patients, many tumors are refractory to such treatments leading in many cases to recurrent or often incurable metastatic disease. This has led to the development of target selective drugs or antibody breast cancer therapies such as herceptin (her2neu; 2). Thus, the identification of proteins, the expression of which is elevated in breast cancer tissues compared with normal breast tissue, is an important first step in the development of future breast cancer therapies.

There have been many studies documenting the use of differential expression analysis to identify mRNAs (3) and proteins (4) that may be relevant to disease states. This is particularly true in the field of oncology where a significant up-regulation in the expression of a protein, coupled with some degree of tissue specificity, can more rapidly identify candidates for therapeutic intervention and diagnostics than for more complex diseases such as obesity and schizophrenia. Differential mRNA expression analysis in clinical breast cancer in particular has been comprehensively studied through the use of DNA microarrays (5–7), with studies becoming more sophisticated through the development of technologies such as laser capture microdissection (8). Proteomic analysis of breast cancer has generated substantially less data due partly to limited access to the relevant technologies as well as the complex sample processing required to generate homogeneous reproducible protein extracts (9). However, proteomics enables the direct analysis of the major effectors (proteins) of changes in cellular behavior. Thus, we have used the cellular sorting systems developed by Page *et al.* (9) who used two-dimensional (2D) gel analysis and mass spectrometry to compare changes in protein expression between normal breast epithelial cells and breast cancer cells.

One of the most consistently up-regulated proteins from our study was arylamine *N*-acetyltransferase-1 (NAT-1), the expression of which was elevated in invasive ductal carcinoma (IDC) and invasive lobular carcinoma (ILC) compared with normal breast. NAT-1 is an enzyme that catalyzes the transfer of an acetyl group from acetyl-CoA to the terminal nitrogen of hydrazine and arylamine drugs or carcinogens (10). Although there have been numerous studies describing the association of NAT-1 polymorphisms with enzyme activity and the development of cancers, there has been few reports of somatic changes in NAT-1 levels associated with cancer progression (11, 12). Given the prevalence of NAT-1 overexpression in this relatively small number of clinical samples, we extended our proteome observations and used real-time quantitative reverse transcription (RT)-PCR and immunohistochemical analysis on clinical

Received 3/31/03; revised 7/10/03; accepted 7/14/03.
The costs of publication of this article were defrayed in part by the payment of page charges. This article must therefore be hereby marked advertisement in accordance with 18 U.S.C. Section 1734 solely to indicate this fact.
Requests for reprints: Jonathan A. Terrett, Oxford Glycosciences (UK) Ltd., 10 The Quadrant, Abingdon Science Park, Abingdon, Oxon, OX14 3YS, United Kingdom. Phone: 44-1235-207687; Fax: 44-1235-207670.
E-mail: jon.terrett@ogs.co.uk

breast cancer donor tissues to assess the normal tissue distribution and cancer prevalence of NAT-1 and association with a known breast cancer prognostic factor, estrogen receptor (ER) status. Furthermore, the association of NAT-1 polymorphisms with cancer and its known role in the metabolism of carcinogens suggested that the observed up-regulation in breast cancer may have functional significance. We therefore investigated the functional significance of elevated NAT-1 on breast epithelial cell growth by overexpressing NAT-1 in the HB4a normal breast epithelium-derived cell line and using a number of assays designed to measure oncogenic potential. The NAT-1-overexpressing cells showed increased resistance to etoposide and were better able to grow in low-serum growth media. Thus, the overexpression of NAT-1 in clinical breast cancers could contribute to the overall carcinogenic process.

Results

Discovery of NAT-1 in Breast Cancer Proteome

A 2D gel analysis was used to compare the proteome of normal breast tissue epithelial cells and breast carcinoma cells. Among a number of observable changes in protein expression patterns on 2D gels between 8 normal breast samples and 25 breast cancer-derived samples was a protein spot at M_r 32,500 that was present in the majority of clinical breast cancer samples and the BT20 breast cancer-derived cell line, but very weak or absent in clinical normal breast samples. Representative examples of the same portion of the 2D gels from normal breast and breast cancer samples indicating the differential protein spot are shown in Fig. 1A. This protein was identified as NAT-1 by SEQUEST correlation of two tandem spectra: (R)LTEENGFWYLDQIR, rawC 1.442, deltaCn 0.412 and (K)NIFNISLQR, rawC 2.013, deltaCn 0.183 which uniquely identify NAT-1. The predicted molecular weight of NAT-1 is M_r 33,000 consistent with this spot representing the full-length NAT-1 protein. Fig. 1B shows the NAT-1 protein spot volumes derived from the 2D proteome of the 8 normal breast, 21 breast carcinoma [13 IDC, 4 ILC, 2 ductal carcinoma *in situ* (DCIS), 1 medullary, and 1 mucinous], and 4 pleural effusion samples compared in the study. Highest NAT-1 spot volumes were seen in the IDC and ILC samples (Fig. 1B).

NAT-1 Messenger RNA Is Up-Regulated in Breast Cancer

NAT-1 mRNA levels were measured by real-time quantitative RT-PCR in a range of normal tissues and breast cancer/normal matched tissues (Fig. 2). These data demonstrate that NAT-1 mRNA is expressed at low levels in multiple normal tissues, with only kidney showing significant levels similar to the BT20 breast cancer-derived cell line where NAT-1 was identified proteomically (Fig. 2A). However, the highest levels of NAT-1 mRNA were found in three of seven clinical breast cancer samples (7398T, 21994T, 20929T) which also show the greatest increase in NAT-1 expression over their adjacent normal breast tissue (Fig. 2B). This correlates well with a larger sample of 40 breast tumor RNAs and 7 normal breast RNAs where 21 of the tumors showed 3-fold elevation or greater NAT-1 mRNA expression *versus* a normal breast mean (data not shown).

Immunohistochemical Analysis of NAT-1 in Breast Cancer

A total of 108 breast tumors was divided into four groups, 44 being ER- and node-positive, 36 ER-positive and node-negative, 13 ER-negative and node-positive, and 15 ER- and node-negative. Additionally, 15 cases of normal breast tissue that had originated from non-tumor-related breast reduction mammoplasties were stained for NAT-1. Analysis of NAT-1 immunostaining shows a significant ($P = 0.004$, Table 1) association of staining intensity with the ER-positive tumors (Fig. 3, A and B); however, the percentage of cells staining for NAT-1 was not significantly associated with ER status. Furthermore, there was no association with NAT-1 tumor staining and their metastatic status. For all 15 normal breast donor tissues, the levels of intensity and percentage of cells staining for NAT-1 within lobules (Fig. 3C) were found to be similar to the ER-negative tumor cells, whereas the surrounding myoepithelia of the lobules were negative.

Overexpression of NAT-1 in a Normal Breast Cell Line

To investigate the biological effect of expressing NAT-1 in normal breast epithelial cells, we created a cell line overexpressing the NAT-1 protein. We chose the conditionally immortalized HB4a human mammary luminal epithelial cell line. HB4a cells retain many features of a normal epithelial phenotype, exhibiting a typical well-organized epithelial morphology (13). HB4a cell growth is slow (doubling time of ~60 h), is inhibited by cell-cell contact, and requires culture medium supplemented with insulin, hydrocortisone, and cholera toxin. The cell line also has a normal phenotype when assayed for transformation, both *in vitro* and *in vivo*, failing to form foci in soft agar and failing to give rise to tumors in nude mice (14). The clonal HB4a/NAT-1 line was generated by transfecting cells with a bicistronic expression vector where the NAT-1 open reading frame and selectable marker were linked by an internal ribosome entry sequence (Fig. 4A). A control cell line, HB4a/Vector, was generated by transfecting HB4a cells with an empty bicistronic expression vector.

To determine whether the HB4a/NAT-1 cell line was expressing active NAT-1 protein, we measured NAT-1 activity in cell lysates using *para*-aminobenzoic acid (PABA) substrate as described in "Patients and Methods." This demonstrated high levels of NAT-1 activity in the HB4a/NAT-1 cell line relative to the HB4a/Vector control cell line (Fig. 4B).

Overexpression of NAT-1 Results in Enhanced Cell Growth and Resistance to Etoposide

To determine the effect of NAT-1 expression on the growth of HB4a cells, HB4a/NAT-1 and HB4a/Vector cells were plated at a density of ~20% in 384-well plates and allowed to attach for 24 h. Images of each well were captured every 2 h for a period of 4 days and the number of living cells [*i.e.*, propidium iodide (PI)-negative] determined for each time point. In a complete medium containing 10% serum, the HB4a/NAT-1 cell line proliferated more quickly than the control HB4a/Vector cell line (Fig. 5A) with a 2-fold increase in the number of NAT-1-expressing cells after 96 h. When the serum concentration

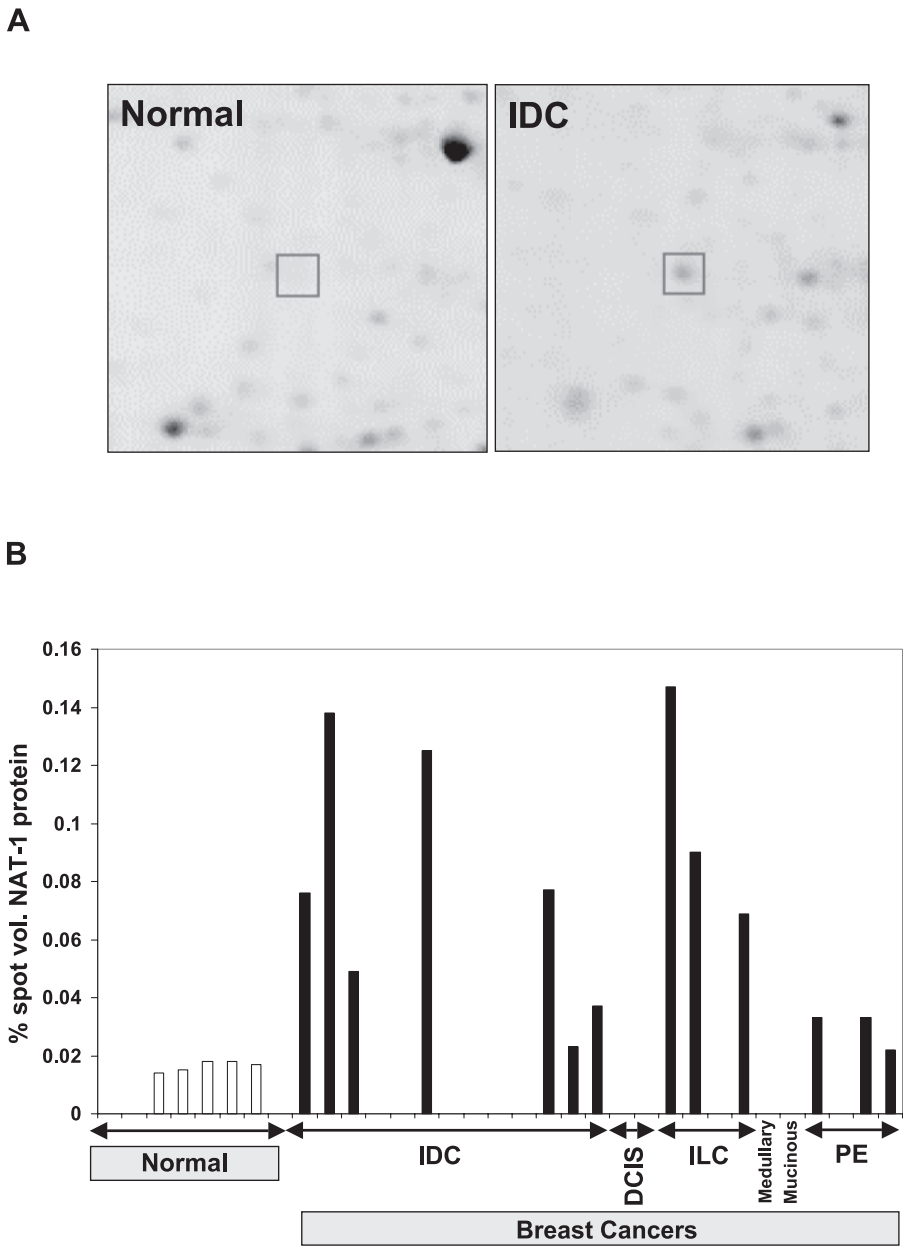

FIGURE 1. Proteomic identification of elevated NAT-1 in breast cancer samples. **A.** Representative examples of the same region of 2D PAGE gels used to resolve normal breast tissue (*Normal*) and IDC epithelial tissue are shown. The protein showing a greater spot volume in the IDC sample compared with the normal sample is indicated (*boxed*). Extraction from the gel, proteolysis, and tandem mass spectrometry determined that this protein was NAT-1. **B.** Spot volume analysis of NAT-1 protein from 2D proteome gels comparing eight normal breast epithelial samples (*Normal*) and multiple clinical breast carcinoma-derived epithelial samples [13 IDC, 2 DCIS, 4 ILC, 1 medullary and 1 mucinous carcinoma, and 4 pleural effusions (*PE*)].

was reduced to 0.5%, the control HB4a/Vector showed no increase in cell number over 96 h; however, the HB4a/NAT-1 cells continued to proliferate and had doubled in population over 96 h (Fig. 5B).

To determine whether expression of NAT-1 could alter the apoptotic response of HB4a cells, we treated the cell lines with the apoptotic agent etoposide. The rate of cell death was tracked in real time through the uptake of PI from the culture medium. HB4a/NAT-1 and HB4a/Vector cells were plated at a density of ~20% in 384-well plates and allowed to attach for 24 h. Cell death was induced by addition of 0.1, 10, and 100 μM etoposide. Images of each well were captured every 2 h for a period of 96 h and the number of dead cells (*i.e.*, PI-positive) determined for each time point. At a dose of 0.1 μM etoposide, there was no significant difference in the level of cell death between the HB4a/NAT-1 and HB4a/Vector cell lines (Fig. 6A). However, at doses of 10 and 100 μM etoposide, there was a marked reduction in the level of dead NAT-1-expressing cells compared with the control cells (Fig. 6, B and C). The drop in the number of PI-positive cells seen for the control cells in Fig. 6C is likely due to the fact that all of the cells per well had died by this time point (~48 h) and thus no further PI was being taken up.

Discussion

In this study, comparative 2D proteomic analysis of multiple clinical normal and breast cancer tissues identified

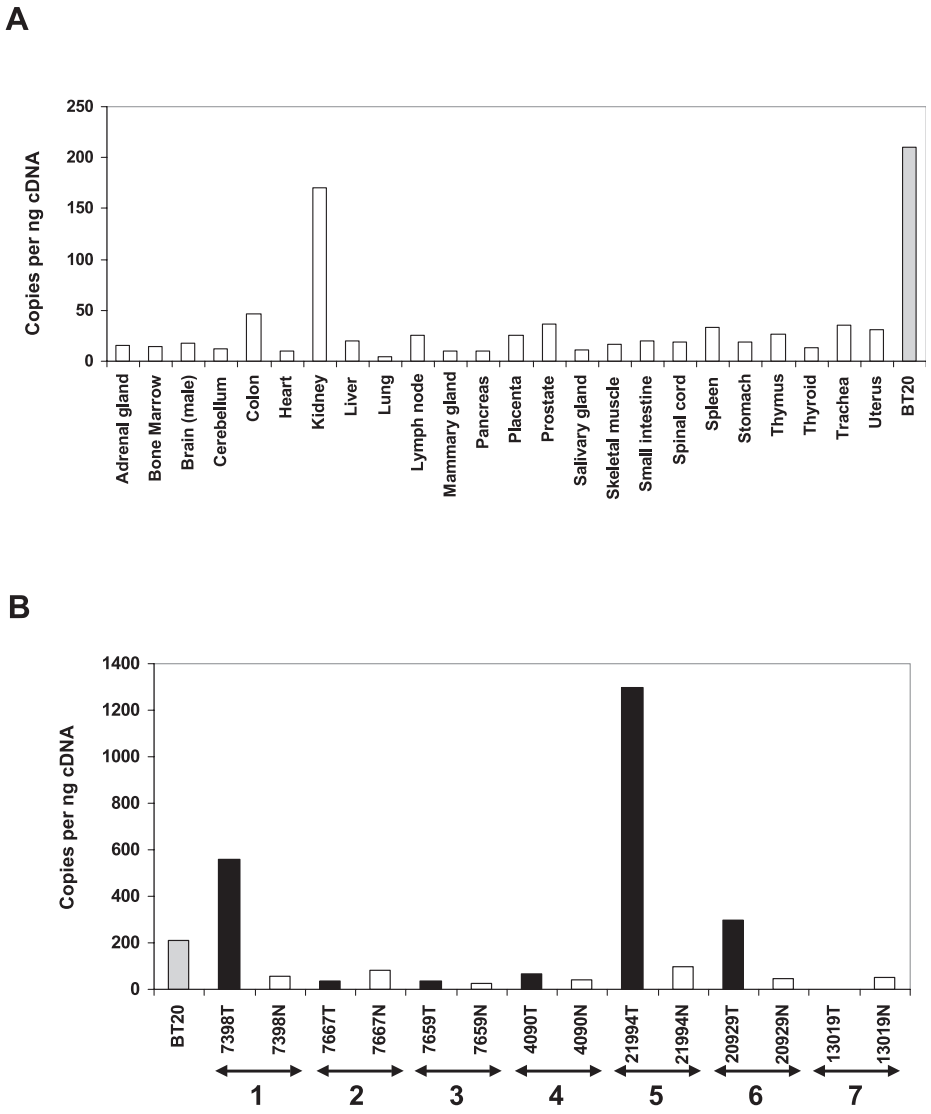

FIGURE 2. Expression of NAT-1 mRNA in normal and breast cancer tissues. Real-time quantitative RT-PCR analysis was used to determine NAT-1 mRNA levels in multiple normal tissues (**A**) and clinical breast adjacent normal/tumor tissues from seven donors (indicated *1–7*; **B**), and the BT20 cell line. Normal tissues are represented by *white bars*, tumor tissues by *black bars*, and the BT20 breast tumor-derived cell line is represented by a *gray bar*. The values shown are means from three separate experiments.

elevated NAT-1 protein in IDC and ILC. This was confirmed at the mRNA level and immunohistochemical analysis of NAT-1 in 108 breast cancer donors demonstrated a strong association of NAT-1 staining with ER-positive tumors. Analysis of the effect of active NAT-1 overexpression in a normal luminal epithelial-derived cell line demonstrated enhanced growth properties and etoposide resistance relative to control cells.

The primary proteomic analyses identified elevated NAT-1 protein in IDC and ILC samples but not in DCIS, medullary, or mucinous cancers. However, these histological definitions of breast cancer seem to be much less relevant to NAT-1 expression than the molecular correlation with ER status. Indeed, Perou *et al.* (15) have also shown evidence of increased NAT-1 mRNA expression in ER-positive breast cancers via DNA microarray analyses. Curiously, we demonstrated that expression levels of NAT-1 in breast cancer-derived cell lines are discordant with ER status where the ER-positive cell lines T47D and MCF7 express less NAT-1 than the ER-negative cell lines BT20 and MB-MDA-468. This suggests that although there is a strong clinical association in expression of NAT-1 and ER, NAT-1 is not dependent on ER expression. As ER status is such a well-characterized prognostic factor for breast cancer, the co-expression of NAT-1 with ER may further define breast cancer prognosis, and indeed, NAT-1 status shows some separation of prognosis in ER-positive breast cancers.[1]

To obtain an as pure as possible population of normal and tumor tissue-derived epithelial cells for our comparative proteome studies, we had to disaggregate the cells for several hours in a collagenase-containing solution before immunomagnetic sorting. One of the consequences of this approach is that both the 'unlinking' of the cells from their stromal microenvironment followed by the processing required to obtain a pure

[1]S. R. Lakhani, personal communication.

Table 1. NAT-1 Expression in Breast Cancer Correlates With ER Status

	Cytoplasmic Intensity			
	0	1	2	3
ER −ve	2	14	9	3
ER +ve	2	17	26	35
Total	4	31	35	38

Note: Immunohistochemical analysis of NAT-1 was examined in 108 breast cancer donor tissues. Intensity of NAT-1 cytoplasmic immunostaining was scored from 0 (no staining) to 3 (strongest staining) for each specimen. In addition, immunohistochemistry was used to score each donor specimen for the presence (ER +ve) or absence (ER −ve) of estrogen receptor nuclear staining. These data demonstrate a strong correlation between ER +ve tumor epithelial cells and high-intensity NAT-1 staining. χ^2 P value 0.004

cell population are likely to change the proteome content of the cells. Nevertheless, tumor and normal samples were treated in the same way, thus ensuring that any changes in proteome content during processing of the tissues were consistent between samples, an important factor for minimizing false positives in comparative 2D analysis, something that could not have been avoided if the epithelial cells had not been purified from contaminating cell types. Moreover, having identified differentially expressed proteins using this proteome approach, we then confirmed their differential expression in clinical normal *versus* tumor epithelial cells in their respective tissue microenvironments using immunohistochemistry.

NAT-1 overexpression induces two of the hallmark traits of cancer, that is, enhanced growth and resistance to toxic compounds. It is unclear how NAT-1 achieves these oncogenic effects, particularly as etoposide is not a recognized substrate for NAT-1, so it seems likely that they are indirect, possibly via aberrant transcription of other genes as a result of increased NAT-1 protein itself or as a secondary effect of increased acetyl transferase activity. Some clues could be gained from comparisons of the mRNA expression profiles of the parental and NAT-1-overexpressing HB4a cells. Furthermore, there is recent evidence from studies of tissue-specific NAT-1 gene expression that there are multiple alternatively spliced NAT-1 transcripts under the control of different transcription factors (16, 17). This suggests the possibility that there are specific NAT-1 transcripts that are elevated in breast tumor tissues due to the presence of high levels of a tumor cell-associated transcription factor.

Despite the potentially indirect oncogenic effects of NAT-1 *in vitro*, the highly prevalent increased expression of NAT-1 in clinical breast cancer needs to be addressed. NAT-1 (and NAT-2) polymorphisms have been found to be important modifiers of pro-carcinogenic substances that were shown to be strongly associated with several common malignancies. Low activity of NAT-2 enzyme is associated with urinary bladder cancer risk, especially in subjects exposed to benzidine (or related arylamines) and to tobacco smoke (18). On the other hand, the rapid NAT-2 and NAT-1 enzymes were implicated as risk factors for colorectal cancer through bioactivation of heterocyclic amines that are present in high concentration in cooked meat (19). A significant association between smoke-induced lung cancer and NAT-1 genotypes has also been described (20). Stanley *et al.* (21) describe elevated NAT-1 expression in well-differentiated human bladder cancers and speculated that aromatic amines are

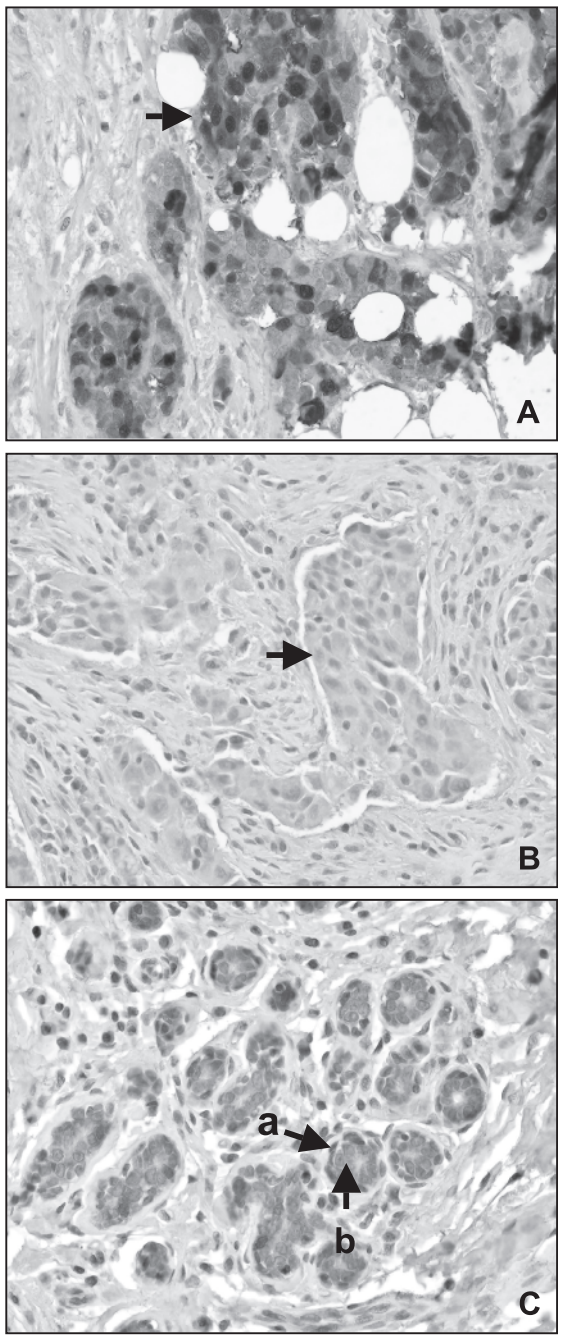

FIGURE 3. NAT-1 immunostaining in breast tissues. **A.** ER-positive primary breast tumor having a high percentage of tumor cells strongly stained for NAT-1 (*arrow*, example tumor cell). **B.** ER-negative primary breast tumor having only weak NAT-1 staining (*arrow*, example tumor cell). **C.** Normal breast tissue lobules (*arrowed b*) having weak NAT-1 staining, the myoepithelia of which (*arrowed a*) are negative. Magnification, ×120.

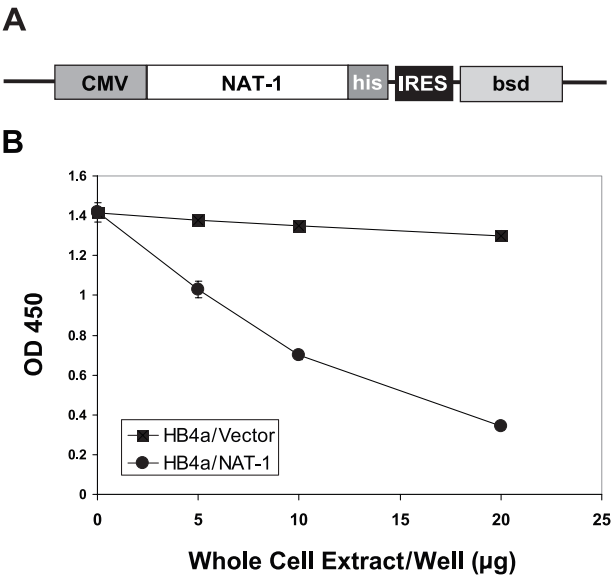

FIGURE 4. Generation of HB4a cell lines overexpressing active NAT-1. **A.** Diagram illustrating the pIRES/NAT-1 construct used to generate the NAT-1-overexpressing HB4a cell line. **B.** Comparison of relative NAT-1 activities in extracts from the HB4a/NAT-1 and HB4a/Vector cell lines. Relative NAT-1 activity is proportional to a decrease in $A_{450\ nm}$. *Points,* means from five separate experiments; *bars,* SE.

metabolized in the bladder epithelium. Furthermore, NAT-1 protein and activity have been identified in normal human mammary epithelial cells where it is thought to be involved in N-hydroxylated heterocyclic amine activation (22).

Because NAT-1 shows associations with carcinogenesis via both polymorphisms and somatic changes in mRNA and protein expression, it remains a challenge to determine how these observations could be used clinically. There may be a prognostic component to NAT-1/ER-positive breast cancers but of more interest is whether modulating NAT-1 activity can contribute to controlling breast cancers. Although our findings demonstrate a high prevalence in breast cancers and oncogenic properties *in vitro* suggest that NAT-1 may be a target for therapy, the finding that NAT-1 mRNA shows highest normal tissue expression in the kidney is an issue which needs to be addressed when considering potential toxicity of NAT-1 therapies. However, the mRNA levels of NAT-1 in the kidney are significantly less than in the highest NAT-1-expressing clinical tumor samples, suggesting that therapeutic doses could be administered which minimize any potential renal toxicity.

Patients and Methods

Tumor Samples and Cell Cultures

Breast tumor donor tissues and normal breast samples obtained from reduction mammoplasties were obtained with full patient consent (John Radcliffe Hospital, University of Oxford, United Kingdom). Histological analysis was carried out on these samples to exclude the possibility of coincidental malignancy or significant benign pathology. Tumor samples were from surgical resections after material had been taken for diagnosis. Tumor tissue used in this study was processed within 3.5 h of resection and held on ice after collection. All tumors were examined and classified by the same experienced breast cancer pathologist. The histopathological criteria used to classify tumors were those recommended by the UK National Health Service Breast Screening Pathology Group (23).

All patients were treated according to unit protocols. All cases had previously been treated at the John Radcliffe Hospital and the Churchill Hospital, Oxford, United Kingdom and all cases underwent either modified radical mastectomy or lumpectomy with breast irradiation for primary treatment. Axillary lymph node-positive cases also received adjuvant radiotherapy to the axillary region. Adjuvant systemic treatment consisted of endocrine therapy (for all post-menopausal women regardless of hormonal receptor status and comprising Tamoxifen at 20 mg daily for 5 years) or chemotherapy (comprising six cycles of i.v. cyclophosphamide, methotrexate, and 5-fluorouracil delivered every 3 weeks). All patients were assessed by follow-up every 3 months for the first 18 months and then every 6 months thereafter. Treatment for confirmed recurrent disease was by endocrine therapy for soft tissue or skeletal metastasis or by chemotherapy for visceral disease and failed endocrine therapy.

Preparation of Purified Cells From Clinical Samples

Normal luminal epithelial cells were prepared from disaggregated reduction mammoplasty tissue by multistage immunomagnetic sorting as we previously described (9). Immunostaining with myoepithelial and luminal-specific lineage markers showed the final sort of luminal epithelial cells used in this study to be 95% pure. Malignant epithelial cells were enriched from disaggregated tumor tissue as follows. Fresh tissue was diced and incubated in 0.25% collagenase (Sigma Type1) in L-15 medium with 2% FCS for 4–6 h with shaking. After brief settling, the supernatant was decanted from large debris, spun down, and the pellet resuspended in L-15 medium and passed through a 100-μm mesh filter. Material passing through consisted mainly of small clusters of epithelial cells and single cells. These were pelleted and if significant red cell contamination was present, this was removed by a 10-min treatment with red cell lysis buffer (Sigma-Adrich LTD., Poole, England). Reactive stromal cells were depleted by pelleting the above preparation, resuspending in L-15 with 10% FCS, and treating with mouse monoclonal antibody F19 to Fibroblast Activation Protein bound to sheep anti-mouse coated Dynabeads (Dynal, United Kingdom). Cells attached to beads were removed with a Dynal MP40 magnet. F19-negative cells were counted and assessed for viability by trypan blue exclusion. The criterion for inclusion of a sample in this study was >80% viability, $>5 \times 10^6$ cells present, presence of recognizable malignant epithelial cells, usually as small clusters, and absence of contamination with significant amounts of normal tissue elements such as ducts, acini, or vessel fragments. Malignant cells were purified from pleurodiesis samples by centrifuging the pleural fluid, resuspending the pellet in tissue culture medium (L-15 plus 10% FCS), and allowing mesothelial cells, the major non-malignant contaminant, to attach to a tissue culture plastic substrate for 2 h before decanting and pelleting the tumor cells. All samples were washed 3× with PBS, pelleted, flash frozen, and stored at −70°C before proteomic analysis.

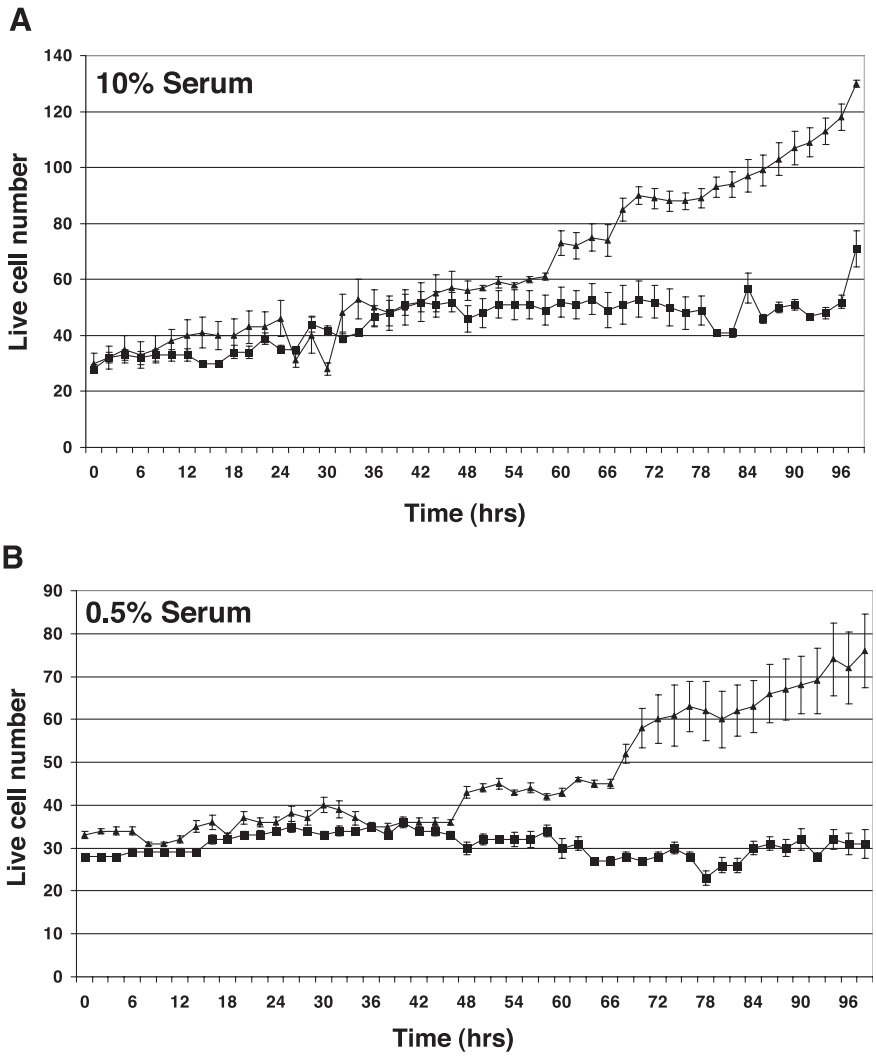

FIGURE 5. NAT-1 overexpression results in enhanced cell proliferation. Growth rates of HB4a/NAT-1 (▲) and HB4a/Vector (■) cell lines were measured in culture media containing 10% (**A**) and 0.5% (**B**) serum. Each *data point* is the average live cell number from triplicate wells at 2 h time points over a period of 96 h.

Proteomic Identification of NAT-1

A 2D gel electrophoresis was performed as previously reported (9). A protein spot at M_r 32,000 was cut from gels containing breast cancer proteins, digested in the gel, and the resulting peptides analyzed using combined MALDI-TOF MS and ESI-MS/MS as previously described (9). Two tandem spectra were identified which matched different tryptic peptides from the NAT-1 protein sequence (Swissprot accession P18440).

Immunohistochemistry

Both primary tumor and normal breast samples were retrieved from the archives of the John Radcliffe Hospital, Oxford, United Kingdom, as formalin-fixed paraffin embedded (FFPE) tissue. All cases had been previously assessed for nodal metastasis. After sectioning, these samples were dewaxed in citroclear (HD Supplies, United Kingdom), rehydrated through graded ethanols to water, and endogenous peroxidases blocked in 3% hydrogen peroxide for 10 min. Tissue antigenicity was achieved by pressure cooking the tissues in target retrieval solution (DAKO, Ely, United Kingdom) for 3 min. Nonspecific IgG binding was blocked using 10% normal human serum in Tris-buffered saline (TBS) for 15 min followed by incubation with the NAT-1 antibody in TBS. Detection was achieved using an Envision kit (DAKO), yielding a dark brown reaction product followed by counterstaining with hematoxylin. Scoring of the cases was done for both levels of intensity, expressed as a number between 0 and 3 (0 being negative and 3 indicating very strong), and for the percentage of tumor cells staining for NAT-1. In the normal cases, ducts, lobules, and their surrounding myoepithelia were scored separately. Node status was defined as positive if the primary breast tumor metastasized to any of the axillary nodes, while ER status was defined as positive if the concentration of ER in the cytosol of tumor cells was greater than 5 μg/ml.

Real-Time Quantitative RT-PCR

Real-time quantitative RT-PCR analysis of gene expression (24, 25) was carried out on first-strand cDNA derived from RNA isolated from samples of breast tumor tissues (John Radcliffe Hospital, University of Oxford, United Kingdom) and normal tissue RNAs (Clontech, Palo Alto, CA). All clinical samples were obtained with informed patient consent and

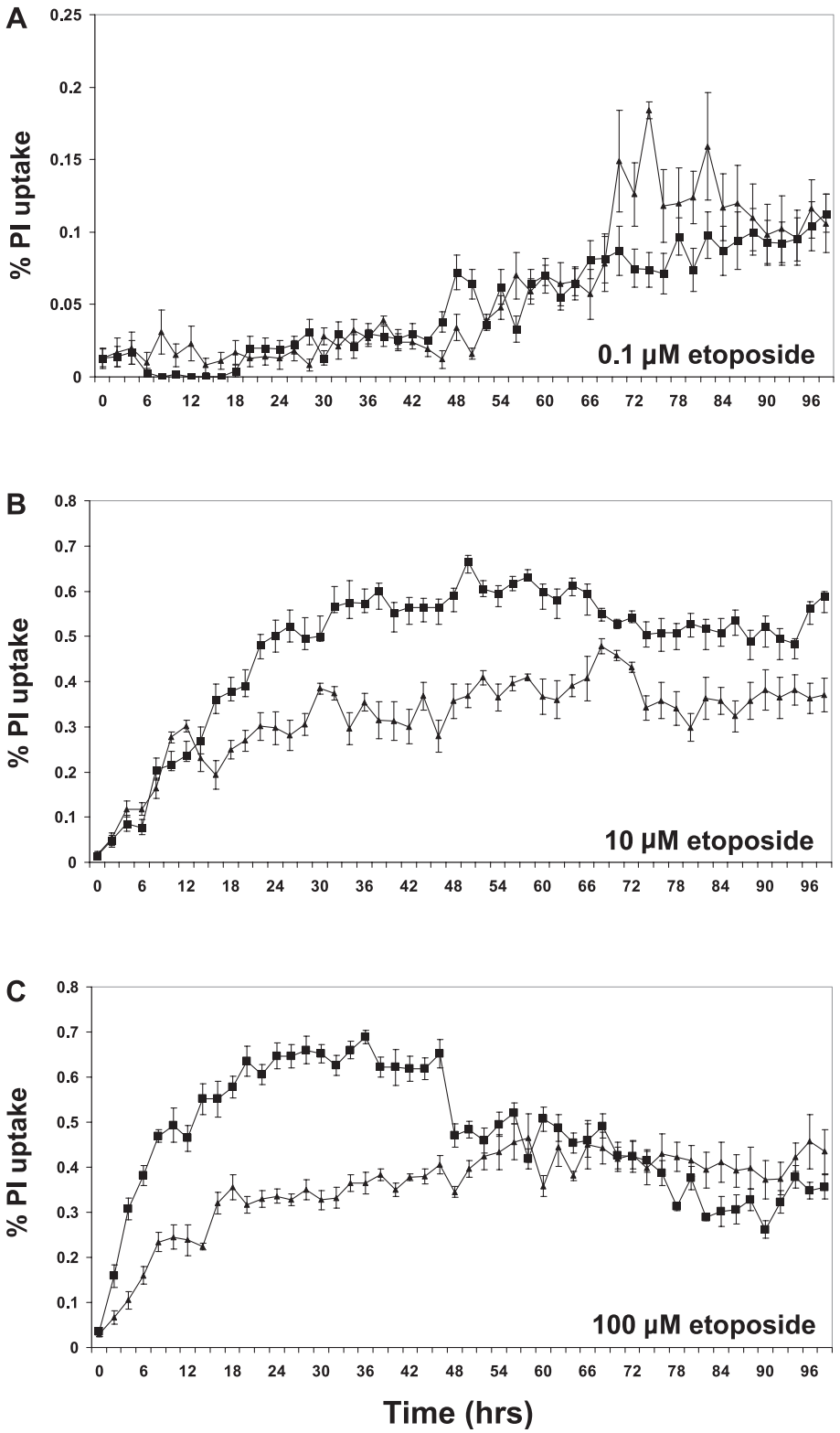

FIGURE 6. NAT-1 overexpression results in resistance to etoposide-mediated cell death. The apoptotic frequency of HB4a/NAT-1 (▲) and HB4a/Vector (■) cell lines was measured after treatment with 0.1 (**A**), 10 (**B**), and 100 μM (**C**) etoposide. Each *data point* is the average percentage of cells staining with PI at each 2 h time point over a period of 60 h.

ethical approval. Each PCR reaction contained 10 ng first-strand cDNA (prepared from each mRNA sample using Superscript reverse transcriptase, Life Technologies, Inc., Carlsbad, CA), SYBR green sequence detection reagents (Applied Biosystems, Foster City, CA), and sense and antisense primers. PCR reactions containing 5 ng cDNA, SYBR green sequence detection reagents (PE Biosystems, Foster City, CA), Taq Polymerase, sense (5′ atacatacctgcagacatctcc 3′), and

antisense (5′ tttgggcacaagctttctctgc 3′) primers were assayed on an ABI 7000 sequence detection system (Applied Biosystems). The PCR conditions were 1 cycle at 50°C for 2 min, 1 cycle at 95°C for 10 min, and 40 cycles at 95°C for 15 s, 65°C for 1 min. The accumulation of PCR product was measured in real time as the increase in SYBR green fluorescence. Standard curves relating initial template copy number to fluorescence and amplification cycle were generated using the amplified, sequence-confirmed PCR product as a template, and were used to calculate copy number in each sample. Data were analyzed and NAT-1 copies per nanogram cDNA values were calculated for each tissue examined using the Sequence Detector program v1.6.3 (Applied Biosystems).

Generation of Recombinant NAT-1 Overexpressing HB4a Cell Line

The HB4a cell line was derived by infection of human breast epithelial cells with a retrovirus expressing a temperature-sensitive mutant of SV40 large T-antigen (13). HB4a cells and derivatives were cultured in RPMI medium (Invitrogen, Carlsbad, CA), supplemented with 10% fetal bovine serum, 2 mM L-glutamine, 5 μg/ml hydrocortisone, 5 μg/ml insulin, and 10 ng/ml cholera toxin. Cell lines were maintained in a humidified atmosphere in 5% CO_2 at 37°C. The expression vector pIRESbsd was constructed by inserting the blasticidin resistance gene (*bsd*) into the *Xba*I and *Not*I sites downstream of the internal ribosome entry sequence of pIRES (Clontech). A bicistronic vector (pIRESbsd-NAT-1) expressing NAT-1 protein was constructed by inserting the open reading frame of NAT-1 into the *Nhe*I and *Eco*RI sites located upstream of the internal ribosome entry sequence in pIRESbsd. DNA was prepared using UltraMobius purification (Novagen, Madison, WI) and linearized with *Hpa*I before transfection. HB4a cells were transfected on 60-mm dishes with linearized expression vector using Fugene-6 transfection reagent (Roche, Basel, Switzerland). Forty-eight hours after transfection, the cell culture media were supplemented with blasticidin at 5 μg/ml. When selection was completed, HB4a cells were kept as a polyclonal population and maintained in 5 μg/ml blasticidin. The drug-resistant colonies were then isolated using cloning cylinders (Sigma) and cell numbers expanded for Western analysis. HB4a clones were maintained in 5 μg/ml blasticidin and passage minimized.

Phenotypic Assays of Proliferation and Cell Death

Proliferation and cell death assays were performed by Automated Cell, Incorporated (ACI, Pittsburgh, PA) using their Phenotype-Driven Discovery Technology. One day before initiating the assay, cells were plated to yield a density of 20% on the following day. The cells were plated so that each culture condition was represented by triplicate wells on a single 384-well plate. At the start of the assay, culture medium was replaced with experimental cell culture medium containing the appropriate concentration of serum or etoposide. Fetal bovine serum was used at 10%, 2.5%, and 0.5% v/v with the concentrations of insulin, hydrocortisone, and cholera toxin remaining the same as in normal complete growth medium. For drug-induced apoptosis experiments using etoposide, the etoposide was added to give a final concentration of 100, 10, or 0.01 μM in culture medium containing 10% serum but lacking additional survival factors (insulin, hydrocortisone, and cholera toxin). PI was added to the culture medium at 1 μg/ml as a fluorescent marker of cell death. Cells were transferred to the ACI Phenotype-Driven Discovery System where visible and fluorescent images were captured every 30 min in each well under 10× magnification. Assay plates remained in the humidified, 5% CO_2 atmosphere at 37°C with constant imaging for 4 days. Images were analyzed using the proprietary ACI Phenotype-Driven Discovery Technology image analysis software where acquired images were pooled and sampled at 2 h intervals.

NAT-1 Activity Assay

NAT-1 activity was assayed using PABA as substrate. Ten microliters of each assay buffer [50 mM Tris (pH 8.0), 1 mM EDTA, 1 mM DTT], 600 μM PABA, and 2.5 mM acetyl-CoA were added to a 96-well plate. The reaction was started by addition of 10 μl enzyme preparation and allowed to proceed at room temperature for 30 min. The reaction was stopped by the addition of 40 μl ice-cold trichloroacetic acid and developed by the addition of 120 μl DMAB (5% dimethylaminobenzaldehyde, 90% acetonitrile, 10% water). The plate was incubated for 5 min at room temperature and then absorbance measured at 450 nm on a Victor2 plate reader (Wallac, Milton Keynes, United Kingdom) with increasing NAT-1 activity being proportional to a decrease in $A_{450\ nm}$. To analyze relative NAT-1 activity in cells, cells were grown to 70% confluency in T175 cm^2 flasks. Lysates were prepared by resuspending PBS washed cells in PBS/1 mM DTT and freeze/thawing three times. Cleared lysates were titrated in the above assay.

References

1. Greenlee, R. T., Murray, T., Bolden, S., and Wingo, P. A. Cancer statistics, 2000. CA Cancer J. Clin., *50:* 7–33, 2000.

2. Brenner, T. L. and Adams, V. R. First MAb approved for treatment of metastatic breast cancer. J. Am. Pharm. Assoc. (Wash.), *39:* 236–238, 1999.

3. DeRisi, J., Penland, L., Brown, P. O., Bittner, M. L., Meltzer, P. S., Ray, M., Chen, Y., Su, Y. A., and Trent, J. M. Use of a cDNA microarray to analyse gene expression patterns in human cancer. Nat. Genet., *14:* 457–460, 1996.

4. Brichory, F., Beer, D., Le Naour, F., Giordano, T., and Hanash, S. Proteomics-based identification of protein gene product 9.5 as a tumor antigen that induces a humoral immune response in lung cancer. Cancer Res., *61:* 7908–7912, 2001.

5. Symmans, W. F., Ayers, M., Clark, E. A., Stec, J., Hess, K. R., Sneige, N., Buchholz, T. A., Krishnamurthy, S., Ibrahim, N. K., Buzdar, A. U., Theriault, R. L., Rosales, M. F., Thomas, E. S., Gwyn, K. M., Green, M. C., Syed, A. R., Hortobagyi, G. N., and Pusztai, L. Total RNA yield and microarray gene expression profiles from fine-needle aspiration biopsy and core-needle biopsy samples of breast carcinoma. Cancer, *97:* 2960–2971, 2003.

6. Adeyinka, A., Emberley, E., Niu, Y., Snell, L., Murphy, L. C., Sowter, H., Wykoff, C. C., Harris, A. L., and Watson, P. H. Analysis of gene expression in ductal carcinoma *in situ* of the breast. Clin. Cancer Res., *8:* 3788–3795, 2002.

7. van't Veer, L. J., Dai, H., van de Vijver, M. J., He, Y. D., Hart, A. A., Mao, M., Peterse, H. L., van der Kooy, K., Marton, M. J., Witteveen, A. T., Schreiber, G. J., Kerkhoven, R. M., Roberts, C., Linsley, P. S., Bernards, R., and Friend, S. H. A gene-expression signature as a predictor of survival in breast cancer. Nature, *415:* 530–536, 2002.

8. Zhu, G., Reynolds, L., Crnogorac-Jurcevic, T., Gillett, C. E., Dublin, E. A., Marshall, J. F., Barnes, D., D'Arrigo, C., Van Trappen, P. O., Lemoine, N. R., and Hart, I. R. Combination of microdissection and microarray analysis to identify gene expression changes between differentially located tumour cells in breast cancer. Oncogene, *22:* 3742–3748, 2003.

9. Page, M. J., Amess, B., Townsend, R. R., Parekh, R., Herath, A., Brusten, L., Zvelebil, M. J., Stein, R. C., Waterfield, M. D., Davies, S. C., and O'Hare, M. J. Proteomic definition of normal human luminal and myoepithelial breast cells

purified from reduction mammoplasties. Proc. Natl. Acad. Sci. USA, *96:* 12589–12594, 1999.

10. Weber, W. W. and Hein, D. W. N-acetylation pharmacogenetics. Pharmacol. Rev., *37:* 25–79, 1985.

11. Bell, D. A., Badawi, A. F., Lang, N. P., Ilett, K. F., Kadlubar, F. F., and Hirvonen, A. Polymorphism in the *N*-acetyltransferase 1 (NAT1) polyadenylation signal: association of NAT1*10 allele with higher N-acetylation activity in bladder and colon tissue. Cancer Res., *55:* 5226–5229, 1995.

12. Badawi, A. F., Hirvonen, A., Bell, D. A., Lang, N. P., and Kadlubar, F. F. Role of aromatic amine acetyltransferases, NAT1 and NAT2, in carcinogen-DNA adduct formation in the human urinary bladder. Cancer Res., *55:* 5230–5237, 1995.

13. Stamps, A. C., Davies, S. C., Burman, J., and O'Hare, M. J. Analysis of proviral integration in human mammary epithelial cell lines immortalized by retroviral infection with a temperature-sensitive SV40 T-antigen construct. Int. J. Cancer, *57:* 865–874, 1994.

14. Harris, R. A., Eichholtz, T. J., Hiles, I. D., Page, M. J., and O'Hare, M. J. New model of ErbB-2 over-expression in human mammary luminal epithelial cells. Int. J. Cancer, *80:* 477–484, 1999.

15. Perou, C. M., Sorlie, T., Eisen, M. B., van de Rijn, M., Jeffrey, S. S., Rees, C. A., Pollack, J. R., Ross, D. T., Johnsen, H., Akslen, L. A., Fluge, O., Pergamenschikov, A., Williams, C., Zhu, S. X., Lonning, P. E., Borresen-Dale, A. L., Brown, P. O., and Botstein, D. Molecular portraits of human breast tumours. Nature, *406:* 747–752, 2000.

16. Butcher, N. J., Arulpragasam, A., Pope, C., and Minchin, R. F. Identification of a minimal promoter sequence for the human arylamine *N*-acetyltransferase 1 gene that binds AP-1 and YY-1. Biochem. J., in press, 2003.

17. Boukouvala, S., Price, N., Plant, K. E., and Sim, E. Structure and transcriptional regulation of the Nat2 gene encoding for the drug metabolising enzyme arylamine *N*-acetyltransferase type 2 in mice. Biochem. J., in press, 2003.

18. Schnakenberg, E., Ehlers, C., Feyerabend, W., Werdin, R., Hubotter, R., Dreikorn, K., and Schloot, W. Genotyping of the polymorphic *N*-acetyltransferase (NAT2) and loss of heterozygosity in bladder cancer patients. Clin. Genet., *53:* 396–402, 1998.

19. Roberts-Thomson, I. C., Ryan, P., Khoo, K. K., Hart, W. J., McMichael, A. J., and Butler, R. N. Diet, acetylator phenotype, and risk of colorectal neoplasia. Lancet, *347:* 1372–1374, 1996.

20. Abdel-Rahman, S. Z., El-Zein, R. A., Zwischenberger, J. B., and Au, W. W. Association of the NAT1*10 genotype with increased chromosome aberrations and higher lung cancer risk in cigarette smokers. Mutat. Res., *398:* 43–54, 1998.

21. Stanley, L. A., Coroneos, E., Cuff, R., Hickman, D., Ward, A., and Sim, E. Immunochemical detection of arylamine *N*-acetyltransferase in normal and neoplastic bladder. J. Histochem. Cytochem., *44:* 1059–1067, 1996.

22. Williams, J. A., Stone, E. M., Fakis, G., Johnson, N., Cordell, J. A., Meinl, W., Glatt, H., Sim, E., and Phillips, D. H. *N*-acetyltransferases, sulfotransferases and heterocyclic amine activation in the breast. Pharmacogenetics, *11:* 373–388, 2001.

23. Pathology Reporting in Breast Cancer Screening (2nd Edition). NHSBSP ISBN 1 87 1997 22 4.

24. Heid, C. A., Stevens, J., Livak, K. J., and Williams, P. M. Real time quantitative PCR. Genome Res., *6:* 986–994, 1996.

25. Morrison, T. B., Weis, J. J., and Wittwer, C. T. Quantification of low-copy transcripts by continuous SYBR Green I monitoring during amplification. Biotechniques, *24:* 954–958, 1998.

Molecular Cancer Research

Arylamine *N*-Acetyltransferase-1 Is Highly Expressed in Breast Cancers and Conveys Enhanced Growth and Resistance to Etoposide *in Vitro*

Paul J. Adam, Joanne Berry, Julie A. Loader, et al.

Mol Cancer Res 2003;1:826-835.